Available online at www.sciencedirect.com
SCIENCE DIRECT
Cement and Concrete Research 35 (2005) 51–55
CEMENT AND CONCRETE RESEARCH

X-ray photoelectron spectroscopy of aluminium-substituted tobermorite

Leon Black[a,*], Andreas Stumm[a], Krassimir Garbev[a], Peter Stemmermann[a], Keith R. Hallam[b], Geoffrey C. Allen[b]

[a]Forschungszentrum Karlsruhe GmbH (ITC-WGT), Hermann-von-Helmholtz-Platz 1, 76344 Eggenstein-Leopoldshafen, Germany
[b]University of Bristol, Interface Analysis Centre, 121 St. Michael's Hill, Bristol BS2 8BS, England

Received 8 March 2004; accepted 9 August 2004

Abstract

We have synthesised 11-Å tobermorite hydrothermally, both pure and with increasing isomorphic substitution of aluminium for silicon. The samples were analysed by X-ray photoelectron spectroscopy (XPS). Aluminium was found, on the basis of its Al 2p binding energies, to be tetrahedrally coordinated. We observed no changes in Ca/(Si+Al) ratio upon aluminium substitution, implying that charge balancing does not occur via the incorporation of additional calcium into the tobermorite structure. Aluminium substitution into the silicate structure led to a decrease in Si 2p binding energies. This implies one of two alternatives. Firstly, that charge balancing occurs via substitution of OH^- for O^{2-} in the tobermorite structure. Secondly, the presence of aluminium in the tobermorite structure may negatively influence the degree of silicate polymerisation. Further work is required to determine which of these possibilities is the case.

Keywords: Crystal structure; Characterization; XPS; Tobermorite; Aluminium substitution

1. Introduction

The particular interest in the structure and crystal chemistry of the tobermorite group of minerals arises from their close relationships with the C–S–H (calcium silicate hydrates) phases formed during the hydration process of Portland cement [1]. Five members of the tobermorite group have been characterised: clinotobermorite, 9-Å tobermorite, 10-Å tobermorite, 11-Å tobermorite and 14-Å tobermorite. The notations 9, 10, 11 and 14 Å refer to the characteristic basal spacings (001-peaks in the XRD patterns) of 9.3, 10.0, 11.3 and 14.0 Å, respectively.

The tobermorite minerals belong to the class of inosilicates, the main structural unit being the wollastonite-type "Dreierkette" [2]. Our interest focuses on 11-Å tobermorite, which comprises calcium- and silicon-layers plus a so-called interlayer [3]. The calcium layer consists of edge-linked seven-fold coordinated calcium polyhedra, running parallel to (001) [4], whilst the silicate layers are formed by double chains, "Dreierdoppelketten", the result of condensation of two wollastonite-type "Dreiereinfachketten" running along *b*. Calcium and silicate layers alternate along *c*-axis connected via shared oxygen atoms. The double chains alternating in the [210] direction are translated by 1/2 along *b*, giving rise to eight-ring channels running along [100]. Within the channels, additional Ca (zeolitic calcium) and water may be placed, leading to the term "interlayer", and allowing possible variations in calcium content.

Aluminium can be incorporated into the structure of 11-Å tobermorite, and aluminium enriched tobermorites may occur in hydrothermally cured cements and aerated concrete. Aluminium substitutes for silicon in the bridging tetrahedra which form the double chains (Q3) [5], although additional substitution in non-bridging tetrahedra has been proposed [6,7]. Considering both the compositions of natural tobermorites and the Loewenstein rule, aluminium substitution for silicon is possible up to Al/(Al+Si)=1/6, with charge compensation via substitution of OH^- for

* Corresponding author. Current Address: Materials and Engineering Research Institute, Sheffield Hallam University, Howard Street, Sheffield, S1 1WB, UK.
E-mail address: l.black@shu.ac.uk (L. Black).

0008-8846/$ - see front matter © 2004 Elsevier Ltd. All rights reserved.
doi:10.1016/j.cemconres.2004.08.005

O^{2-}. Thus, the chemical composition may vary from $Ca_{4.5}Si_6O_{16}(OH)\cdot 5H_2O$ (the most common composition of tobermorite) in "pure" tobermorite, to $Ca_{4.5}AlSi_5O_{15}(OH)_2\cdot 5H_2O$ in the fully exchanged tobermorite. Additionally, there is the possibility of charge balance by varying the calcium content: $Ca_4Si_6O_{15}(OH)_2\cdot 5H_2O$–$Ca_5AlSi_5O_{16}(OH)\cdot 5H_2O$. Charge balance is achieved via coupled substitution $\square+OH^-\rightarrow Ca^{2+}+O^{2-}$, whereby □ indicates the so-called 'empty' position.

A technique ideally suited for examining changes in the bonding and structure materials is X-ray photoelectron spectroscopy (XPS) and thorough reviews of the technique's capabilities may be found elsewhere [8,9]. XPS has been used many times for the study of cement systems [10–14], but few of these have been structural examinations. We have recently used XPS to characterise the different silicate structures within the various C–S–H phases [15–17].

Wagner et al. [18] examined the relationships between the structures of various silicates and their photoelectron spectra. They illustrated how binding energies increased with increasing silicate polymerisation. Furthermore, they showed how incorporation of aluminium into silicate structures led to a decrease in silicon binding energies, due to the increased negative charge introduced into the structure upon substitution of Si^{4+} by Al^{3+}. Similar behaviour was observed by Seyama and Soma [19] for a variety of silicate and aluminosilicate minerals.

This short article examines how photoelectron spectroscopy can be used to examine aluminium incorporation into 11-Å tobermorite. Other articles, using other analysis methods (e.g. XRD, IR, TGA, NMR), to investigate the structures further, are to follow.

2. Experimental

2.1. Sample synthesis

Five samples were prepared from CaO (lime), $Al(OH)_3$ (Fluka) and SiO_2 (Aerosil, Merck) with a water to solid ratio (w/s) of 20, target Ca/(Si+Al) molar ratios of 5/6, and Al/(Al+Si) molar ratios of 0, 1/64, 1/12, 1/9 and 1/6. All syntheses were performed under nitrogen to avoid sample carbonation. The starting materials were treated mechanochemically for 32 h, according to the method of Saito et al. [20] and Sasaki et al. [21]. The resultant nanocrystalline phases were then treated hydrothermally in Teflon-lined steel autoclaves at 170 °C for 22 h followed by an additional 2 h at 180 °C to yield crystalline 11-Å tobermorite. The products were filtered, washed with double-distilled, decarbonated water and dried at 60 °C. Samples were then packed under inert gas prior to analysis. X-ray diffraction was used to confirm 11-Å tobermorite formation and exclude the presence of unreacted starting materials.

2.2. Sample analysis

Prior to XPS analysis, sample purity was confirmed by X-ray diffraction. This was performed using silicon-doped (NIST640b) samples on a D5000 diffractometer from Bruker-AXS employing Cu $K\alpha_{1,2}$ radiation and a graphite secondary monochromator. The measurements were performed in reflection mode over the 2Θ range 2–80° with a 0.02° step and 31 s/step.

XPS analysis was performed on each sample as received, the powders simply being pressed onto adhesive-backed copper tape before introduction into the vacuum chamber. Analysis was performed using a VG Escascope fitted with a MgK_α ($h\nu$=1253.6 eV) X-ray source operating at 260 W (13 kV, 20 mA). After an initial wide spectrum, regional spectra were recorded with a 30-eV pass energy for the important elemental lines (Si 2p, Al 2p, Ca 2p, O 1s and C 1s).

Data were extracted from the spectra via peak fitting using XPSPeak software (available by download from: http://www.phy.cuhk.edu.hk/~surface/). A Shirley background and an 80:20 Gaussian/Lorentzian peak shape were assumed in all cases. Spectra were corrected for charging effects against the adventitious carbon peak at 284.8 eV.

3. Results and discussion

A qualitative evaluation of the X-ray diffraction patterns confirmed that the samples are phase-pure with some negligible amounts of calcium carbonate, calcite and aragonite, and the zeolitic aluminosilicate, ferrierite (Fig. 1). No traces of gibbsite were found, confirming the incorporation of aluminium into the tobermorite structure. The slight changes in the position of the (002) reflection revealed enlargement of the c parameter with increasing aluminium content, also confirming aluminium incorporation [22].

3.1. XPS spectra

3.1.1. Ca 2p spectra

Aluminium incorporation does not affect the Ca 2p binding energies (Table 1). All the samples showed Ca $2p_{3/2}$ binding energies of approximately 346.9 eV, compared to ~346.8 eV for calcite and portlandite. There is only a weak relationship between C–S–H structure and Ca 2p binding energy dependent upon silicate anion type, phyllosilicates having higher Ca 2p binding energies than other silicate anion types [15]. Thus, in this study, only concerned with 11-Å tobermorite, an inosilicate, a trend in binding energies would not be expected.

We have already stated that charge balancing upon incorporation of aluminium may be achieved by increasing the calcium content. As all of our samples were prepared from starting materials with the same Ca/(Al+Si) ratio, then the aluminium-poor samples may be expected to contain an excess of calcium, most probably present as calcium

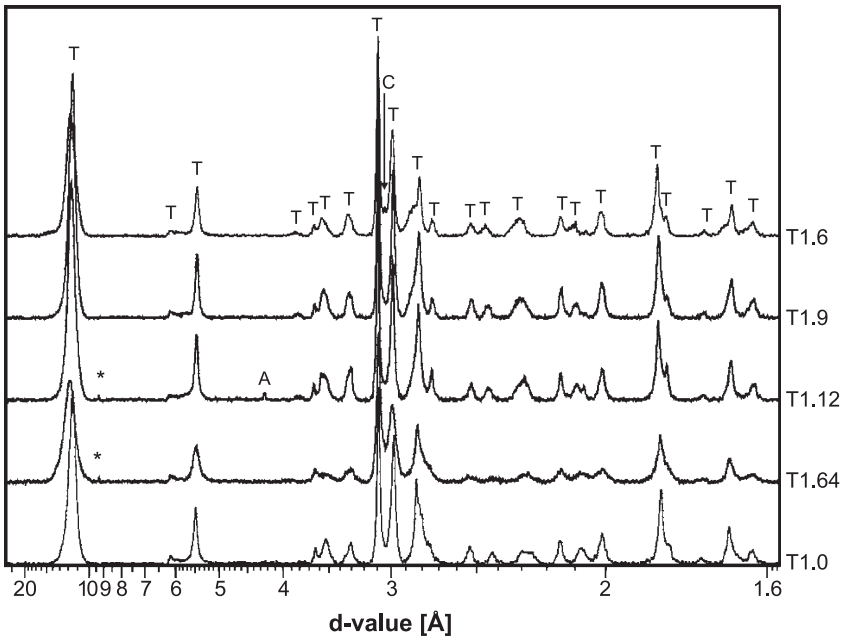

Fig. 1. X-ray diffraction patterns of the aluminium-substituted 11-Å tobermorite samples. T=tobermorite, C=calcite, A=aragonite; *possibly ferrierite.

carbonate. Thus, to determine whether charge balancing occurred via changes in calcium content, we must examine the Ca/(Si+Al) ratios of the 11-Å tobermorite phase and look for the presence of calcium carbonate.

We observed no changes in the Ca/(Si+Al) ratios of the 11-Å tobermorite phase with increasing aluminium content, either by XPS or EDX analysis during examinations by environmental scanning electron microscopy (details not shown). Similarly, the diffraction patterns showed no systematic variation in carbonate content. It appears therefore that charge balancing does not occur via changes in calcium content. To confirm this, we looked for evidence of calcium carbonate formation. The Ca $2p_{3/2}$ binding energies of the three possible $CaCO_3$ polymorphs are 346.8, 347.0 and 347.3 eV[1] for vaterite, calcite and aragonite, respectively [23]. These values are similar to the values for 11-Å tobermorite. However, the presence of carbonate should still be detectable via a C 1s peak at approximately 289.5 eV. We did not find any evidence for major changes in the carbonate contents of our samples, confirming that charge balancing does not occur via changes in the calcium content.

3.1.2. Si 2p spectra

Fig. 2 shows the variation in Si 2p binding energies and peak widths with increasing aluminium content. Aluminium incorporation leads to a decrease in Si 2p binding energy. The decrease is evident for Al/(Al+Si)>1/64, and even then is only slight, but it is consistent. However, care is needed when interpreting this trend. The error in the binding energy values is ±0.05. Thus, it is uncertain as to whether this decrease is linear or that there is a step for Al/(Al+Si)≥1/9. The consequences of each of these alternatives are described below.

Barr et al. [24] reported a shift to lower Si 2p binding energies for sheet silicates with increasing Al/Si. Seyama and Soma [19] observed similar behaviour in the Si 2s binding energies of various aluminosilicate minerals. Substitution of Al^{3+} for Si^{4+} results in an effective increase in the negative charge on the silicate anion, increased shielding of the silicon nuclei, and thus a decrease in binding energy. In this instance, an approximately linear decrease in binding energy with increasing aluminium content would be expected, and substitution of OH^- for O^{2-} would be the charge compensation mechanism.

Alternatively, a stepped decrease in the Si 2p binding energies could be explained by a reduction in the number of double silicate chains in the silicate structure upon aluminium incorporation. A lower degree of polymerisation leads to lower silicon binding energies [15,16,25]. According to Faucon et al. [26–28] increasing aluminium content leads to breaking of the silicate chains to form $[Si_2O_7]$ groups. A drawback of the model of Faucon et al. is that the

Table 1
Details of important spectral data

Binding energy (eV)	0	1/64	1/12	1/9	1/6
Si 2p	101.90	101.90	101.88	101.81	101.78
FWHM	2.34	2.56	2.39	2.38	2.41
Ca $2p_{3/2}$	346.90	346.90	346.90	346.89	346.91
FWHM	2.07	2.18	2.04	2.06	2.12
δ_{Ca-Si}	245.00	245.00	245.02	245.08	245.13
Al 2p	–	–	74.12	73.97	73.92
FWHM	–	–	2.45	1.84	2.82

[1] Note that we have corrected all of our binding energies against a binding energy for the adventitious carbon peak of 284.8 eV. Other groups may use slightly different values for this carbon peak. Where this is so, we have re-calculated the literature values for consistency.

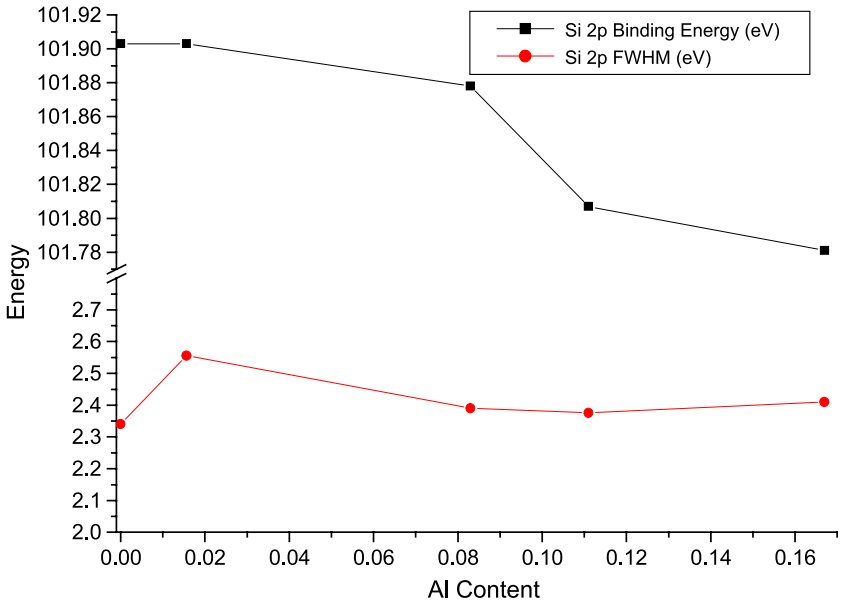

Fig. 2. Si 2p binding energies and FWHM with increasing aluminium content, Al/(Al+Si).

authors used the structural model of Hamid [29], which is based on the presence of "dreiereinfachketten", and not dreierdoppelketten" as found in many ^{29}SiNMR or IR studies.

In addition to the decrease in binding energies, incorporation of aluminium leads to a broadening of the Si 2p peaks. Even ignoring the apparent outlier for Al/(Al+Si)=1/64 the increase upon incorporation is significant at the 5% level. Different bonding environments lead to differences in binding energy, therefore peak broadening indicates the presence of silicon atoms in various different electronic environments, namely **Si**–O–Si and **Si**–O–Al species. Another cause could be the presence of silanol (**Si**–OH) groups. However, analysis by NMR spectroscopy showed no evidence of silanol groups in these samples.

Additionally, a careful examination of the powder diffraction patterns reveals broadening of the diffraction peaks in this sample, indicating a slightly less crystalline sample. This will also lead to broadening of the photoelectron peaks.

3.1.3. Al 2p spectra

Aluminium was only detected by XPS for Al/(Al+Si)>1/12, even then the peaks were weak and determination of the precise binding energies was difficult. The binding energies were approximately 74 eV, but fell slightly from 74.12 eV for Al/(Al+Si)=1/12 to 73.92 eV for Al/(Al+Si)=1/6.

Barr et al. reported that aluminium binding energies are dependent upon coordination number. Tetrahedrally coordinated aluminium generally has a lower binding energy than octahedrally coordinated aluminium, i.e. 73.4–74.55 and 74.1–75.0 eV, respectively [30]. Despite the overlap in these regions, our values of 74.1 eV and below appear to indicate tetrahedrally coordinated aluminium in 11-Å tobermorite, as expected. A decrease in binding energies with increasing aluminium substitution was also observed by Seyama and Soma [19], who concluded that decreases in both Si 2p and Al 2p binding energies was attributable to charge delocalisation over the entire silicate anion.

3.1.4. O 1s spectra

We observed no difference in the O 1s spectra with increasing aluminium content. We had hoped to see changes in the spectra due to the presence of Si–O–Al species, similar to those seen for pure C–S–H phases upon changes in the ratio of bridging (Si–O–Si) to non-bridging (Si–O–Ca) oxygen atoms [15,31]. However, the electronegativity of aluminium lies between that of calcium and silicon, thus the binding energies of Si–O–Al species lie between those of the bridging and non-bridging oxygen atoms. Our spectral resolution was not sufficient to distinguish between these different groups.

Similarly, the changes in the O 1s spectrum expected if charge balancing was achieved via substitution of OH^- for O^{2-} are too slight to be resolved in this experiment. The presence of an additional OH group, at the expense of a non-bridging oxygen atom would lead to only a very slight change in the O 1s spectrum. The situation is complicated further by the presence of an indeterminable amount of water of crystallisation.

4. Conclusions

Isomorphic substitution of aluminium for silicon into the silicate structure of 11-Å tobermorite leads to a decrease in Si 2p binding energies. Substitution of Al^{3+} for Si^{4+} ions leads to increased shielding of the silicon atoms and thus lower binding energies. Conversely, following the model of Faucon et al. [26–28], the observed trends may also be due to lower silicate polymerisation upon aluminium incorpo-

ration. However, as no changes were observed in the Ca/(Si+Al) ratios nor in the levels of calcium carbonate present upon aluminium substitution, the possibility of charge balancing by additional calcium in aluminium-substituted 11-Å tobermorite may be excluded.

The aluminium binding energies indicate tetrahedrally coordinated aluminium. Increasing aluminium substitution led to slight decreases in Al 2p binding energies. That both the Si 2p and Al 2p binding energies decreased with increasing substitution indicates that the electrons are delocalised over the silicate anions.

There was no noticeable change in Ca 2p binding energies with increasing aluminium substitution. We suppose that aluminium incorporation does not greatly influence the bonding environment of calcium. Similarly, we observed no differences in the O 1s spectra. This was due however to insufficient spectral resolution when using a laboratory-based machine.

Acknowledgements

We acknowledge the comments of two anonymous referees whose valuable comments and suggestions much improved this article.

References

[1] H.F.W. Taylor, The calcium silicates hydrates, in: H.F.W. Taylor (Ed.), The Chemistry of Cements, Academic Press, London, 1964, pp. 167–232.
[2] F. Liebau, Bemerkungen zur Systematik der Kristallstrukturen von Silikaten mit hochkondensierten Anionen, Phys. Chem. 206 (1956) 73–92.
[3] C. Hoffmann, T. Armbruster, Clinotobermorite, $Ca_5[Si_3O_8(OH)]_2 \cdot 4H_2O$–$Ca_5[Si_6O_{17}] \cdot 5H_2O$, a natural C–S–H (I) type cement mineral: determination of the substructure, Z. Kristallogr. 212 (1997) 864–873.
[4] S. Merlino, E. Bonaccorsi, T. Armbruster, Tobermorite: their real structure and order–disorder (OD) character, Am. Mineral. 84 (1999) 1613–1621.
[5] I.G. Richardson, A.R. Brough, R. Brydson, G.W. Groves, C.M. Dobson, The location of aluminum in substituted calcium silicate hydrate (C–S–H) gels as determined by 29 Si and 27 Al NMR and EELS, J. Am. Ceram. Soc. 76 (1993) 2285–2288.
[6] P. Faucon, J.C. Petit, T. Charpentier, J.F. Jacquinot, F. Adenot, Silicon substitution for aluminum in calcium silicate hydrates, J. Am. Ceram. Soc. 82 (5) (1999) 1307–1312.
[7] S. Komarneni, R. Roy, D.M. Roy, C.A. Fyfe, G.J. Kennedy, A.A. Bothner-By, J. Dadok, A.S. Chesnick, Aluminum-27 and silicon-29 magic angle spinning nuclear magnetic resonance spectroscopy of aluminum-substituted tobermorites, J. Mater. Sci. 20 (11) (1985) 4209–4214.
[8] D. Briggs, M.P. Seah, Practical Surface Analysis, 2nd ed., Auger and X-ray Photoelectron Spectroscopy, vol. 1, Wiley, Chichester, UK, 1994.
[9] M.F. Hochella Jr., Auger electron and X-ray photoelectron spectroscopies, in: F.C. Hawthorne (Ed.), Reviews in Mineralogy, Spectroscopic Methods in Mineralogy and Geology, vol. 18, Mineralogical Society of America, Washington, DC, 1988, pp. 573–637.
[10] S. Long, C. Liu, Y. Wu, ESCA study on the early C_3S hydration in NaOH solution and pure water, Cem. Concr. Res. 28 (2) (1998) 245–249.
[11] D. Ménétrier, I. Jawed, T.S. Sun, J. Skalny, ESCA and SEM studies on early C_3S hydration, Cem. Concr. Res. 9 (1979) 473–482.
[12] M. Regourd, J.H. Thomassin, P. Baillif, J.C. Touray, Study of the early hydration of Ca_3SiO_5 by X-ray photoelectron spectrometry, Cem. Concr. Res. 10 (1980) 223–230.
[13] J.H. Thomassin, M. Regourd, P. Baillif, J.C. Touray, Étude de l'hydratation initiale du silicate bicalcique β par spectrométrie de photo-électrons, C.R. Acad. Sci., Paris 290 (1980 Jan.) 1–3.
[14] M.Y.A. Mollah, T.R. Hess, Y.-N. Tsai, D.L. Cocke, An FTIR and XPS investigations of the effects of carbonation on the solidification/stabilization of cement based systems—Portland type V with zinc, Cem. Concr. Res. 23 (1993) 773–784.
[15] L. Black, K. Garbev, P. Stemmermann, K.R. Hallam, G.C. Allen, Characterisation of crystalline C–S–H phases by X-ray photoelectron spectroscopy (XPS), Cem. Concr. Res. 33 (6) (2003) 899–911.
[16] L. Black, K. Garbev, P. Stemmermann, K.R. Hallam, G.C. Allen, Erratum to "characterisation of crystalline C–S–H phases by X-ray photoelectron spectroscopy (XPS), Cem. Concr. Res. 33 (6) (2003) 899–911;
Cem. Concr. Res. 33 (11) (2003) 1913.
[17] L. Black, A. Stumm, K. Garbev, P. Stemmermann, K.R. Hallam, G.C. Allen, X-ray photoelectron spectroscopy of the cement clinker phases tricalcium silicate and β-dicalcium silicate, Cem. Concr. Res. 33 (10) (2003) 1561–1565.
[18] C.D. Wagner, D.E. Passoja, H.F. Hillery, T.G. Kinisky, H.A. Six, W.T. Jansen, J.A. Taylor, Auger and photoelectron line energy relationships in aluminium–oxygen and silicon–oxygen compounds, J. Vac. Sci. Technol. 21 (4) (1982) 933–944.
[19] H. Seyama, M. Soma, Bonding-state characterization of the constituent elements of silicate minerals by X-ray photoelectron spectroscopy, J. Chem. Soc., Faraday Trans. 81 (1985) 485–495.
[20] F. Saito, G. Mi, M. Hanada, Mechanochemical synthesis of hydrated calcium silicates by room temperature grinding, Solid State Ionics 101–103 (1997) 37–43.
[21] K. Sasaki, T. Masuda, H. Ishida, T. Mitsuda, Synthesis of calcium silicate hydrate with Ca/Si=2 by mechanochemical treatment, J. Am. Ceram. Soc. 80 (1996) 472–476.
[22] S. Diamond, J.L. White, W.L. Dolch, Effects of isomorphous substitution in hydrothermally synthesized tobermorite, Am. Mineral. 51 (1966) 388–401.
[23] C.S. Gopinath, S.G. Hegde, A.V. Ramaswamy, S. Mahapatra, Photoemission studies of polymorphic $CaCO_3$ materials, Mater. Res. Bull. 37 (2002) 1323–1332.
[24] T.L. Barr, E.E. Hoppe, S. Hardcastle, S. Seal, X-ray photoelectron spectroscopy investigations of the chemistries of soils, J. Vac. Sci. Technol., A, Vac. Surf. Films 17 (4) (1999) 1079–1085.
[25] K. Okada, Y. Kameshima, A. Yasumori, Chemical shifts of silicon X-ray photoelectron spectra by polymerization structures of silicates, J. Am. Ceram. Soc. 81 (7) (1998) 1970–1972.
[26] P. Faucon, J.F. Jacquinot, J.M. Delaye, J. Virlet, Molecular dynamics simulation of Al^{3+} and Na^+ substitutions in the tobermorite structure, Philos. Mag., B 75 (1996) 769–783.
[27] P. Faucon, J.M. Delaye, J. Virlet, Molecular dynamics simulation of the structure of calcium silicate hydrates (I): $Ca_{4+x}Si_6O_{14+2x}(OH)_{4-2x}(H_2O)_{0.4\times4}$, J. Solid State Chem. 127 (1996) 92–97.
[28] P. Faucon, J.M. Delaye, J. Virlet, J.F. Jackuinot, F. Adenot, Study of the structural properties of the C–S–H (I) by molecular dynamics simulation, Cem. Concr. Res. 27 (1997) 1581–1590.
[29] S.A. Hamid, The crystal structure of the 11 Å natural tobermorite $Ca_{2.25}[Si_3O_{7.5}(OH)_{1.5}] \cdot 2H_2O$, Z. Kristallogr. 154 (1981) 189–198.
[30] T.L. Barr, S. Seal, K. Wozniak, J. Klinowski, ESCA studies of the coordination state of aluminium in oxide environments, J. Chem. Soc., Faraday Trans. 93 (1) (1997) 181–186.
[31] L. Black, K. Garbev, P. Stemmermann, K.R. Hallam, G.C. Allen, X-ray photoelectron study of oxygen bonding in crystalline C–S–H phases, Phys. Chem. Minerals 31 (2004) 337–346.